

# Beringian origins and cryptic speciation events in the fly agaric (*Amanita muscaria*)

J. GEML,\* G. A. LAURSEN,\* K. O'NEILL,† H. C. NUSBAUM† and D. L. TAYLOR\*

\*Institute of Arctic Biology, 311 Irving I Building, 902 N. Koyukuk Drive, PO Box 757000, University of Alaska Fairbanks, Fairbanks, AK 99775, USA, †Sequence and Analysis Program, Broad Institute, 320 Charles Street, Cambridge, MA 02141, USA

## Abstract

*Amanita muscaria sensu lato* has a wide geographic distribution, occurring in Europe, Asia, Africa, Australia, New Zealand, and North, Central and South America. Previous phylogenetic work by others indicates three geographic clades (i.e. 'Eurasian', 'Eurasian-alpine' and 'North American' groups) within *A. muscaria*. However, the historical dispersal patterns of *A. muscaria* remained unclear. In our project, we collected specimens from arctic, boreal and humid temperate regions in Alaska, and generated DNA sequence data from the protein-coding beta-tubulin gene and the internal transcribed spacer (ITS) and large subunit (LSU) regions of the ribosomal DNA repeat. Homologous sequences from additional *A. muscaria* isolates were downloaded from GenBank. We conducted phylogenetic and nested clade analyses (NCA) to reveal the phylogeographic history of the species complex. Although phylogenetic analyses confirmed the existence of the three above-mentioned clades, representatives of all three groups were found to occur sympatrically in Alaska, suggesting that they represent cryptic phylogenetic species with partially overlapping geographic distributions rather than being allopatric populations. All phylogenetic species share at least two morphological varieties with other species, suggesting ancestral polymorphism in pileus and wart colour pre-dating their speciations. The ancestral population of *A. muscaria* likely evolved in the Siberian–Beringian region and underwent fragmentation as inferred from NCA and the coalescent analyses. The data suggest that these populations later evolved into species, expanded their range in North America and Eurasia. In addition to range expansions, populations of all three species remained in Beringia and adapted to the cooling climate.

**Keywords:** biogeography, coalescent, fungi, nested clade analysis, phylogeography, supertree

Received 22 May 2005; revision received 2 September 2005; accepted 17 October 2005

## Introduction

*Amanita muscaria* (L.: Fr.) Hooker, the 'fly agaric', is probably the most famous and most illustrated fungus and embodies the concept of 'mushroom' in many cultures. Its popularity likely arises from its attractive appearance, wide geographic distribution, and perhaps from its psychoactive properties (Benjamin 1995; Hudler 1998; Michelot & Melendez-Howell 2003). There are several varieties, primarily described to distinguish the different colour forms, such as *A. muscaria* var. *muscaria* (L.: Fr.) Hooker (pileus red, stem and warts white), *A. muscaria* var. *alba* Peck (pileus, warts

and stem white to tan), *A. muscaria* var. *flavivolvata* (Singer) Jenkins (pileus orange to red, warts tannish-yellow, stem white to cream), *A. muscaria* var. *formosa* (Pers.: Fr.) Bertillon in DeChambre (pileus orange to yellow, warts and stem yellowish to tannish), *A. muscaria* var. *persicina* Jenkins (pileus melon, warts tannish to yellowish), and *A. muscaria* var. *regalis* (Fr.) Bertillon in DeChambre (pileus brown, warts tannish to yellowish) (Jenkins 1986). *A. muscaria* is native to temperate or boreal forest regions of the Northern Hemisphere; however, it has been introduced to New Zealand, Australia, South America, and South Africa (Reid 1980; Thiers 1982; Santiago *et al.* 1984; Jenkins 1986; Tan & Wu 1986; Pérez-Silva & Herrera 1991; Reid & Eicker 1991; Ridley 1991; Rimóczi 1994; Tulloss *et al.* 1995; Bhatt *et al.* 2003). It is an ectomycorrhizal

Correspondence: József Geml, Fax: (907) 474 6967; E-mail: jgeml@iab.alaska.edu

(ECM) fungus with a wide host range (Trappe 1962). Although it is most commonly associated with various birch (*Betula*), pine (*Pinus*), spruce (*Picea*), fir (*Abies*) and larch (*Larix*) species, it is known to form ECM associations with representatives of other genera, particularly when its primary hosts are rare or nonexistent in a certain area. For example, after being introduced to the Southern Hemisphere by pine seedlings transported from Europe, it has been observed to form ECM symbioses with native trees, such as *Nothofagus*, *Kunzea* and *Leptospermum* species (Bagley & Orlovich 2004). Also, at least one morphological variety, *A. muscaria* var. *regalis*, occurs above altitudinal tree line in interior Alaska, where it has been found associated with *Dryas* and *Salix* species (Miller 1982).

Prior research in the literature suggests that *A. muscaria* exhibits substantial variation in morphology and toxin content (Benedict 1966; Jenkins & Petersen 1976; Jenkins 1986). Despite the broad awareness of the plasticity of *A. muscaria* across different geographic regions, Oda *et al.* (2004) were the first authors to report on the phylogeny and biogeography of the species complex based on DNA sequence data generated from specimens collected in Japan, Nepal, New Zealand, Norway, Poland, the United Kingdom, and various parts of the United States. They found three distinct clades in *A. muscaria* that they considered 'Eurasian', 'Eurasian subalpine' and 'North American' groups, corresponding to geographic differences (i.e. allopatric populations). They hypothesized that the ancestral group of *A. muscaria* existed only in Eurasia and later migrated to North America via land bridges.

Beringia, including Alaska and northeastern Siberia, has long been a focal point for biogeographic research in a wide range of plant and animal taxa. This high level of interest arises for two principal reasons. First, due to its diverse landscape and climate and the fact that much of the region remained ice-free during glacial maxima, Beringia served as a refugium for arctic and sub-arctic flora and fauna. Second, during much of the Tertiary and the Quaternary periods, Beringia was the major land connection between Asia and North America and provided migration routes to a wide variety of organisms (for example, see Adams & Faure 1997; Qian 1999; Elias 2000; Swanson 2003; Kaufman *et al.* 2004). Despite the importance of the unique biogeographic history of Alaska, no specimen of *A. muscaria* has been investigated from this region. Therefore, our goal was to further elucidate the phylogenetic and phylogeographic structure in *A. muscaria* by collecting and analysing specimens from Arctic, boreal and humid temperate regions in Alaska. We generated DNA sequence data from the protein-coding beta-tubulin gene and the internal transcribed spacer (ITS) and large subunit (LSU) regions of the ribosomal DNA repeat, and conducted comprehensive phylogenetic analyses including homologous *A. muscaria* sequences published by Oda *et al.* (2004). We used genea-

logical concordance as outlined by Taylor *et al.* (2000) to determine phylogenetic species boundaries within *A. muscaria*. We conducted phylogenetic analyses based on individual data sets for each locus, on a combined data set of the three loci, and using a 'phylogenetic supertree' approach (Sanderson *et al.* 1998). In addition, we used nested clade analyses (NCA) (Templeton 1998) to reveal the phylogeographic history of the individual phylogenetic species and the species complex as a whole. To be able to better interpret and place in time the results of the phylogeographic analyses, we estimated the ages of the divergence points of the main clades using molecular clock methods. Also, we conducted coalescent-based simulations of genealogical relationships to further enhance the precision of estimates of population and mutation ages, migration, and mutational structures of ancestral populations (Beerli & Felsenstein 1999; Nielsen & Wakeley 2001; Carbone *et al.* 2004).

## Materials and methods

### *Isolates and DNA extraction*

Twenty specimens were collected from various geographic regions of Alaska (Table 1). Sporocarps were deposited in the University of Alaska Fairbanks (UAF) Mycological Herbarium. DNA was extracted from small samples of dried specimens using the E-Z 96® Fungal DNA Kit (Omega Bio-tek). ITS and beta-tubulin sequences of additional *Amanita muscaria* isolates were downloaded from GenBank (Table 1). Homologous sequences of *Amanita pantherina* (isolate FB-30958) published by Oda *et al.* (2004) were used to root all trees.

### *PCR and DNA sequencing*

A portion of the beta-tubulin gene was amplified in polymerase chain reaction (PCR) mixtures containing 16.5 µL PCR water, 2.5 µL 10 × PCR buffer (0.5 M KCl, 0.1 M Tris-HCl pH 8.3, 0.025 M MgCl<sub>2</sub>), 2.5 µL 10 × dNTPs (2 mM of each dNTP), 0.125 µL *Taq* DNA polymerase (Fisher Scientific), 0.25 µL of 10 µM forward primer and reverse primer, and 1 µL template DNA (original DNA solution extracted). PCR and cycle sequencing reactions were performed in a PTC-220 thermocycler (Programmable Thermal Controller) using primers and settings specified by Oda *et al.* (2004). Amplification products were electrophoresed in a 1.0% agarose gel and stained with ethidium bromide for visualization of the bands. PCR products were purified directly using the QIAquick® PCR Purification Kit (QIAGEN). Purified amplification products were sequenced using the Applied Biosystems (ABI) BigDye® version 3.1 Terminator Kit and an ABI 3100 automated capillary DNA sequencer (PerkinElmer).

**Table 1** *Amanita muscaria* isolates included in the multilocus phylogenetic analyses

	Isolate code*	Origin	GenBank Accession no.			
			ITS	beta-tubulin	LSU	
<i>A. muscaria</i>	GAL2814	Dalton Highway, mile 122, Alaska, USA	DQ060897	DQ060917	DQ060877	
	GAL4302	Juneau, Alaska, USA	DQ060910	DQ060923	DQ060890	
	GAL5895	Nome, Alaska, USA	DQ060898	DQ060918	DQ060878	
	GAL5900	Nome, Alaska, USA	DQ060902	—	DQ060882	
	GAL5946	Nome, Alaska, USA	DQ060903	—	DQ060883	
	GAL8950	Denali National Park, Alaska, USA	DQ060901	—	DQ060881	
	GAL15776	Bonanza Creek LTER site, Alaska, USA	DQ060893	DQ060913	DQ060873	
	30961†	Aomori-shi, Aomori, Japan	AB080980	AB095892	—	
	30962†	Kitakoma-gun, Yamanashi, Japan	AB080981	AB095893	—	
	30963†	Kitakoma-gun, Yamanashi, Japan	AB080982	AB095894	—	
	30976†	Kiso-gun, Nagano, Japan	AB081294	AB095895	—	
	30977†	Ohno-gun, Gifu, Japan	AB081295	AB095896	—	
	30985†	Ohno-gun, Gifu, Japan	AB096048	AB095897	—	
	30978†	Chino-shi, Nagano, Japan	AB081296	AB095858	—	
	30981†	Chino-shi, Nagano, Japan	AB096049	AB095859	—	
	30982†	Chino-shi, Nagano, Japan	AB096050	AB095860	—	
	30964†	Gdynia, Poland	AB080983	AB095899	—	
	30965†	Gdansk, Poland	AB080984	AB095900	—	
	31452†	Hampshire, England, UK	AB080777	AB095901	—	
	31445†	Surrey, England, UK	AB080778	AB095902	—	
	80048†	Surrey, England, UK	AB080779	AB095903	—	
	30987†	Queenstown, New Zealand	AB096052	AB095904	—	
	45843†	Hampshire, Massachusetts, USA	AB080788	AB095884	—	
	45785†	Hampshire, Massachusetts, USA	AB080789	AB095885	—	
	45840†	Lawrence, Massachusetts, USA	AB080791	AB095887	—	
	45820†	Bronx, New York, USA	AB080790	AB095886	—	
	45863†	Mendocino, California, USA	AB080787	AB095883	—	
	<i>A. m. var. alba</i>	GAL14284	Denali National Park, Alaska, USA	DQ060895	DQ060915	DQ060875
		GAL15453	North Pole, Alaska, USA	DQ060899	DQ060919	DQ060879
		GAL16735	Fairbanks, Alaska, USA	DQ060896	DQ060916	DQ060876
		49100†	Cascade, Idaho, USA	AB080793	AB095889	—
	<i>A. m. var. formosa</i>	GAL4247	Juneau, Alaska, USA	DQ060894	DQ060914	DQ060874
		GAL15330	Fairbanks, Alaska, USA	DQ060891	DQ060911	DQ060871
GAL15461		North Pole, Alaska, USA	DQ060900	DQ060920	DQ060880	
GAL16775		Fairbanks, Alaska, USA	DQ060892	DQ060912	DQ060872	
45883†		Piscataquis, Massachusetts, USA	AB080792	AB095888	—	
45060†		Amador, California, USA	AB080795	AB095891	—	
44761†		Alpine, California, USA	AB080794	AB095890	—	
<i>A. m. var. regalis</i>	GAL2810	Dalton Highway, mile 122, Alaska, USA	DQ060904	—	DQ060884	
	GAL3169	Eagle Summit, Alaska, USA	DQ060905	—	DQ060885	
	GAL3688	Juneau, Alaska, USA	DQ060906	—	DQ060886	
	GAL5505	Denali National Park, Alaska, USA	DQ060908	DQ060922	DQ060888	
	GAL6027	Nome, Alaska, USA	DQ060909	—	DQ060889	
	GAL16654	Fairbanks, Alaska, USA	DQ060907	DQ060921	DQ060887	
	506†	Dovre, Oppland, Norway	AB080780	AB095855	—	
	1539†	Gjøvik, Oppland, Norway	AB080781	AB095856	—	
	4220†	Nordre-land, Oppland, Norway	AB080782	AB095857	—	

\*Sequences of isolates marked by † were published by Oda *et al.* (2004).

The entire ITS and partial LSU regions were PCR amplified in reaction mixtures containing 1.75 µL Ultrapure Water (Invitrogen), 1 µL 10 × Herculase PCR buffer (Stratagene), 0.05 µL 100 mM dNTP mixture, 25 mM of each dNTP

(Applied Biosystems), 0.2 µL Herculase DNA polymerase (Stratagene), 2 µL of 1 µM forward primer, ITS1F (Gardes & Bruns 1993) and reverse primer, TW13 (White *et al.* 1990), and 3 µL of template DNA at a concentration of

0.1 ng/ $\mu$ L. PCRs were performed using the following temperature programme for the two ribosomal gene regions: 95 °C/2 min, 34 cycles of 95 °C/0.5 min, 54 °C/1 min, 72 °C/2 min; and 72 °C/10 min. The concentration of the amplification products was determined using Picogreen (Molecular Probes). The amplification products were normalized to a concentration of 4 ng/ $\mu$ L and sequenced using the ABI BigDye version 3.1 Terminator Kit and an ABI 3730xl automated capillary DNA sequencer (Applied Biosystems). Because the amplification products were 1300+ bp long, we used two internal primers for cycle sequencing, ITS4 and CTB6 (White *et al.* 1990), in addition to the primers used in the PCRs.

### *Phylogenetic analysis*

Sequence data obtained for both strands of each locus were edited and assembled for each isolate using CODONCODE ALIGNER version 1.3.4 (LI-COR). Sequence alignments were initiated using CLUSTAL W (Thompson *et al.* 1997) and subsequently corrected manually. Although none of the three loci contained ambiguously aligned positions, a hypervariable region was observed in the beta-tubulin data set corresponding to positions 60–86. These positions could still be aligned across all groups, yet there were a large number of gaps corresponding to a 21-bp deletion and several smaller indels. We recoded this region using INAASE 2.3b (Lutzoni *et al.* 2000) to retain the phylogenetic information present in the region without overweighing the deletions. The code matrix was attached to the alignment and was included in maximum-parsimony (MP) analyses. Analyses were conducted in multiple steps using the MP method in PAUP\* 4b10 (Swofford 2002), and Bayesian analysis in MRBAYES 3.0 (Huelsenbeck & Ronquist 2001). Because the methods above follow different theories and algorithms, only congruent branching patterns found in both types of analyses were considered meaningful. To test the combinability of DNA sequence data from different loci, the partition homogeneity test (PHT) was performed on only parsimony-informative sites with 1000 randomized data sets, using heuristic searches with simple addition of sequences. The best-fit evolutionary model for Bayesian analyses was determined for each data set by comparing different evolutionary models with varying values of base frequencies, substitution types,  $\alpha$ -parameter of the  $\gamma$ -distribution of variable sites, and proportion of invariable sites via the Akaike information criterion (AIC) using PAUP\* and MODELTEST 3.06 (Posada & Crandall 1998). MP analyses were carried out with the heuristic search option using the 'tree-bisection-reconnection' (TBR) algorithm with 100 random sequence additions to find the global optimum with MAXTREES set to 10 000 in the combined analyses. To test the stability of clades detected, the bootstrap test (Felsenstein 1985) was used with 'full heuristic search'. The

number of replicates were 1000 and 100 for the individual and combined data sets, respectively. In Bayesian phylogenetic analyses, 200 000 generations were run in four chains for the single-locus, and 1 000 000 generations for the combined data sets. The chains were sampled every 100th generation. When the likelihood scores of trees sampled approached similar values, they were considered to have converged. In each run, trees after this convergence point were used to compute a majority rule consensus tree. Gaps were scored as 'new state' in MP and as 'missing data' in Bayesian analyses. To compare the likelihood of different tree topologies, two-tailed Kishino–Hasegawa tests were used (Kishino & Hasegawa 1989) with parsimony and likelihood settings specified beforehand.

### *Supertree construction*

We constructed supertrees using the Matrix Representation with Parsimony method (MRP) (Baum 1992; Ragan 1992), a supertree approach for analysing and combining individual trees derived from multiple data sets. One of the biggest advantages of using supertree methods is the ability to combine phylogenetic information present in only partially overlapping data sets (i.e. the ability to overcome missing data). In MRP, the topology of each source tree is recoded as a series of binary characters describing each node. Each character describes a clade in a tree such that descendants of the node are scored as '1', all others as '0' except for missing data that is scored '?'. The resulting matrix is then analysed using parsimony to produce a consensus estimate based on the source trees (Jones *et al.* 2002). MRP handles conflict by weighing the evidence in different source trees without any tree having the power of veto (Creevey & McInerney 2004).

While published supertree analyses have generally been based on pre-existing phylogenies as source trees, we used the Bayesian trees generated earlier in this study for individual loci to construct supertrees. Bininda-Emonds & Sanderson (2001) assessed the accuracy of MRP and concluded that weighted MRP performed at least equally well or better than the total evidence approach (analyses of combined original data sets), and always better than nonweighted MRP. They recommended weighting source trees based on node support, such as bootstrap values, whenever possible. Following this path, but adopting a slightly different approach, we chose 100 random trees for each locus from the sets of trees generated in Bayesian analyses after the convergence of likelihood scores. This enabled us to weight the nodes according to their posterior probability values (i.e. their observed frequencies in the sampled trees). We produced the MRP matrix by combining the matrix representation of all 300 trees in PAUP. MP analyses were carried out with the heuristic search option using the TBR algorithm with 100 random sequence additions. The stability of clades was



evaluated by bootstrap test, resampling nodes as characters, used with 'full heuristic search', and 1000 replicates.

### Phylogeographic analyses

Phylogeographic patterns linked to the different phylogenetic species and the species complex as a whole were investigated using NCA (Templeton 1998). To improve the performance of the NCA, we removed the haplotype representing the sample from New Zealand. Because *A. muscaria* is not native to the Southern Hemisphere, including this isolate would have introduced an unnecessary source of error in the process of inferring the phylogeographic history of the species complex. Maximum-parsimony haplotype networks were generated by TCS version 1.18 (Clement *et al.* 2000) and were used to define a series of nested clades that in turn were used to perform random, two-way contingency permutation analysis to detect any association between geographic distribution and genetic variation (Templeton 1998). The nested clade information, sample size for each haplotype, and geographic location of each clade (latitude and longitude coordinates) were entered into the software package GEODIS version 2.0 (Posada *et al.* 2000). GEODIS was used to calculate clade distance ( $D_c$ ) and nested clade distance ( $D_n$ ), and to test them for significance at  $\alpha = 0.05$  level using a permutation technique with 10 000 resampling replicates (Posada *et al.* 2000).  $D_c$  was calculated as the average distance of all individuals in clade 'X' from the geographic centre of that clade, while  $D_n$  was the average distance of individuals in clade 'X' from the geographic centre of clades of the next highest nesting level. Where significant  $D_c$  and/or  $D_n$  values were detected, a set of criteria was used to detect the effects of contemporary (e.g. gene flow) vs. historical (e.g. allopatric fragmentation, and range expansion) processes (Templeton 1998; Posada *et al.* 2000). In addition, nucleotide diversity ( $\pi$ , the average pairwise nucleotide differences per site) was calculated using ARLEQUIN version 2.0 (Schneider *et al.* 2000) to compare the amount of genetic diversity found in Alaska to that of other geographic groups.

### Coalescent analyses

Identical sequences were collapsed into haplotypes using SNAP MAP (Aylor & Carbone 2003) and SITES version 1.1 (Hey & Wakeley 1997), excluding insertion or deletions (indels) and categorizing base substitutions as phylogenetically uninformative or informative, and transitions vs. transversions. Although coalescent methods can take full advantage of the data, they make strict assumptions, such as neutrality and lack of recombination, that must be verified a priori. Tajima's  $D$  (Tajima 1989) and Fu and Li's  $D^*$  and  $F^*$  (Fu & Li 1993) test statistics were calculated with DNASP version 3.53 (Rozas & Rozas 1999) to test for

departures from neutrality. SNAP Clade and SNAP Matrix (Markwordt *et al.* 2003) were used to generate site compatibility matrices to detect recombination blocks. Based on the evidence for geographic population structure as detected by NCA, MDIV (Nielsen & Wakeley 2001) was used to distinguish equilibrium migration vs. shared ancestral polymorphisms between subdivided populations. MDIV applies Markov chain Monte Carlo (MCMC) coalescent simulations to estimate the population mean mutation rate, divergence time, migration rate, and the time since the most recent common ancestor (TMRCA). Subsequently, we reconstructed the genealogy with the highest root probability, the ages of mutations, and the TMRCA of the sample using coalescent simulations with population subdivision in GENETREE version 9.0 (Griffiths & Tavaré 1994).

### Molecular clock analyses

To estimate the ages of the nodes, maximum-likelihood (ML) analyses were conducted using PAUP\* 4b10 based on LSU sequences, with and without the enforcement of a molecular clock. The data set contained the same taxa with eight additional sequences representing other groups of Basidiomycota (*Ustilago maydis* AF453938, *Auricularia delicata* AF291290, *Boletus pallidus* AF457409, *Stropharia coronilla* AF059232, and *Melanophyllum haematospermum* AF261476). The likelihood values of the resulting trees were compared by the  $\chi^2$ -test at  $\alpha = 0.05$  significance level. The test statistic was equal to twice the difference of log-likelihood scores, which is  $\chi^2$  distributed with  $n - 2$  degrees of freedom, where  $n$  is the number of terminal taxa (Page & Holmes 1998). Absolute ages of nodes were estimated by fixing the age of the *Ustilaginomycetes/Hymenomycetes* separation at 430 million years ago (Ma) (based on Berbee & Taylor 2001). The branch length and standard error values were estimated using PAML (Yang 1997).

## Results

### Phylogenetic analyses

The ITS, beta-tubulin, LSU and the combined data sets consisted of 717, 468, 625, and 1810 characters, respectively, including gaps. There were 36, 14, 12, and 62 parsimony-informative characters, respectively. The Tamura–Nei model (Tamura & Nei 1993), with calculated proportion of invariable sites and equal variation rates for all sites (TrN + I), was selected as the best-fit evolutionary model for all three individual data sets.

In Bayesian analysis of the ITS, beta-tubulin, LSU, and combined data sets, the consensus trees were computed from 1162, 484, 1510, and 5238 trees, after discarding the first 839, 1517, 491, and 4763 trees as 'burn-in', respectively. MP analyses generated 16, 39, 3, and 10 000 equally parsimonious

trees for the ITS, beta-tubulin, LSU, and combined data sets, respectively. The ITS phylograms were 95 steps long with consistency index (CI) = 0.874, retention index (RI) = 0.965, rescaled consistency index (RC) = 0.843, and homoplasy index (HI) = 0.126. Trees generated from the beta-tubulin alignment had the following scores: length = 109 steps, CI = 0.862, RI = 0.840, RC = 0.725, and HI = 0.138. The LSU phylograms were 22 steps long, and had scores of CI = 0.864, RI = 0.906, RC = 0.783, and HI = 0.136. MP trees of the combined data set were 231 steps long with CI = 0.848, RI = 0.925, RC = 0.785, and HI = 0.152.

Three major clades receiving high support (Clades I–III, Fig. 1) were detected within *Amanita muscaria* based on phylogenetic analyses of the ITS and LSU alignments; however, the relationships among Clades I, II, and III were not clear. Although both Clades I and III formed monophyletic groups, only Clade I was well supported in the beta-tubulin phylograms, despite a moderate number of parsimony-informative sites. All three groups had unique 'signature sequences' in the hypervariable region corresponding to positions 60–86 in the alignment. In this region, isolates in Clades I and III were monomorphic within their clades and characterized by a 21-bp deletion in Clade I, and several small indels in Clade III. Although many isolates of Clade II were polymorphic, they all shared a GT (positions 82–83) 'insertion' unique to the clade, and none of them had sequences identical to the two other groups. (This 'insertion' should be interpreted as nucleotides that are missing in both Clades I and III, and does not refer to the evolutionary history of the sites.) While the beta-tubulin MP tree did not support the monophyly of Clade II, it did not show significant conflict with the ITS and LSU trees. When Clades I, II, and III were under monophyletic constraint, the equally parsimonious trees (length = 111, CI = 0.847, RI = 0.819, RC = 0.694, and HI = 0.153) were only two steps longer than the unconstrained trees described earlier. The Kishino–Hasegawa test revealed that the difference between the two topologies was not significant ( $P = 0.48$ ). Apparently, this lack of conflict was not due to low phylogenetic signal in beta-tubulin. A permutation tail probability (PTP) test (Archie 1989; Faith & Cranston 1991) revealed that the beta-tubulin locus contributes phylogenetic signal to the combined data set, because tree length of the original beta-tubulin phylogram was significantly shorter ( $P < 0.01$ ) than the length of the trees generated based on randomly permuted beta-tubulin data sets. As expected, Clades I, II, and III were strongly supported in analyses of the combined data set with 96%, 99%, and 100% MPB and all 1.0 BPP values, respectively (Fig. 1A). A southeast Alaskan subclade (II/A) also received high support: 96% MPB and 1.0 BPP. Phylogenetic relationships among Clades I, II, and III remained unclear, as none of the groupings were supported by significant MPB and BPP values.

### Supertree construction

Matrix representations of the ITS, beta-tubulin, and LSU resulted in 93, 73, and 39 characters (recoded nodes), respectively, for each tree. Therefore, the entire data set containing matrix representations of 100 trees for each locus contained 20 500 characters. Out of these, 9800 characters were parsimony-informative. The single most parsimonious tree (see Supplementary material) was 33 803 steps long with CI = 0.606, RI = 0.743, RC = 0.451, and HI = 0.394. All of the major clades described earlier and subclade II/A were well resolved.

### Evolution of morphological varieties

Representatives of multiple, morphologically distinct varieties were found in several clades. To test whether specimens with shared phenotype were monophyletic, Kishino–Hasegawa tests were performed. Tree length and likelihood score of the most likely of the 10 000 MP trees constructed from the unconstrained combined data set were compared to the length and likelihood scores of the most likely MP tree under the constraint of monophyly of the morphological variety in question. Separate analyses were conducted for each morphological variety to detect whether any one of the three *A. muscaria* varieties (var. *alba*, var. *formosa*, and var. *regalis*) was monophyletic. Other varieties were not tested, because for many isolates only the species identity was known, without reference to the variety, making it impossible to distinguish between the two varieties with red pileus: *A. muscaria* var. *muscaria* (often referred to only by species name) and *A. muscaria* var. *flavivolvata*. In all analyses, the constrained trees were significantly worse (i.e. had significantly more steps and lower likelihood scores) than the unconstrained trees (all  $P < 0.01$ ) (Table 2).

### Phylogeographic analyses

A total of 25 haplotypes were detected in *A. muscaria* isolates from the Northern Hemisphere (Fig. 2). Although these haplotypes grouped in three separate networks at 95% connection limit, representing the major clades described earlier, it was possible to connect these clades at 92% connection limit. The nested haplotype networks of Clades I, II, and III are shown in Fig. 2. Haplotypes XII, I, and XXIII were inferred to have the highest outgroup probability in the separate cladograms representing Clades I, II, and III, respectively. In the total cladogram connecting all clades, haplotype I had the highest outgroup probability. The missing intermediate haplotypes were retained during the nesting procedure for consistency in nesting (Crandall 1996).

In the network of Clade I, the null hypothesis of no association between genotype and geographic origin was

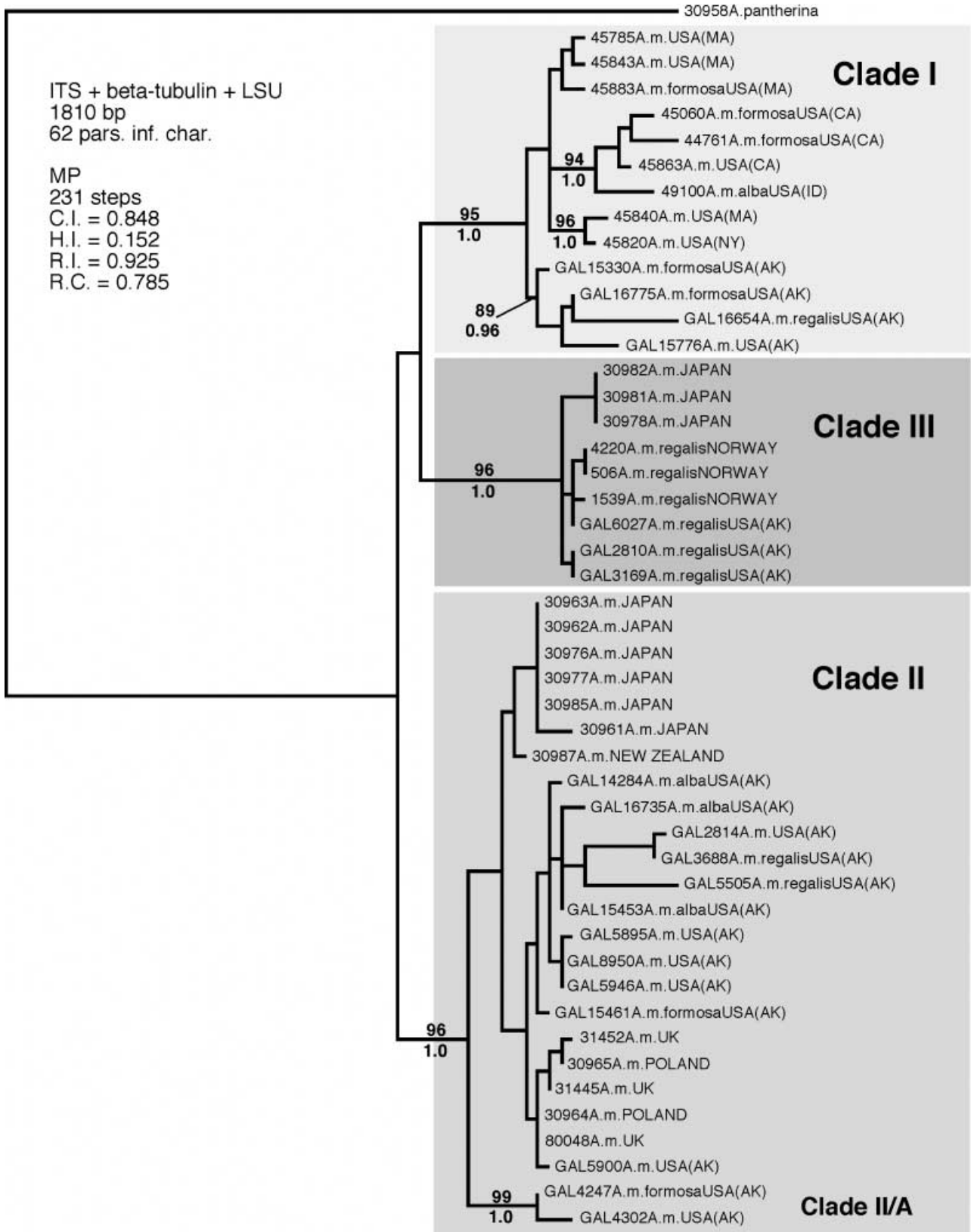
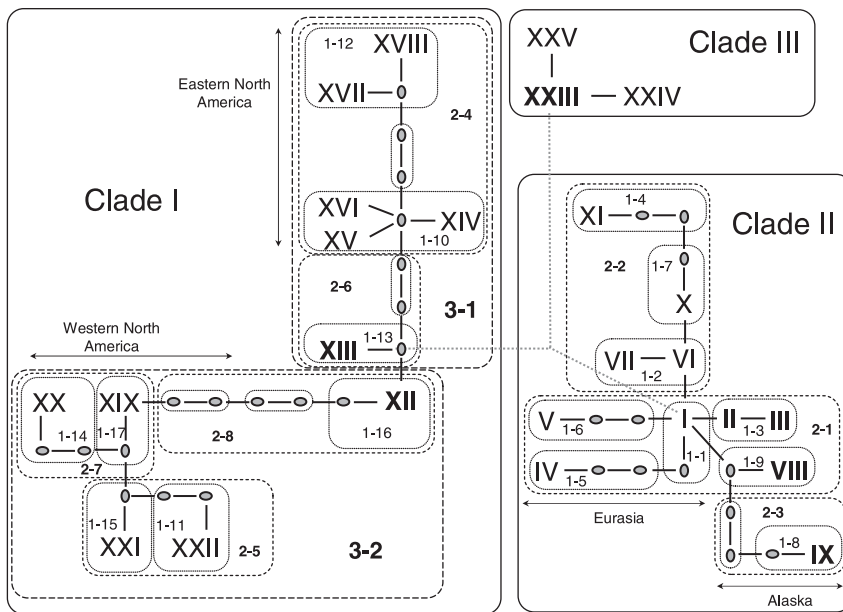


Fig. 1 One of the 10 000 equally parsimonious trees for the combined data set with >70% maximum-parsimony bootstrap and >0.95 Bayesian posterior probability values shown above and below the supported branches, respectively.

**Table 2** Results of Kishino–Hasegawa tests for monophyly of morphological varieties based on maximum-parsimony analyses of the combined data set

Morphological variety	Tree	–ln L	Diff. –ln L	<i>P</i>	No. of steps	Diff. no. of steps	SD	<i>t</i>	<i>P</i>
	unconstrained	3476.1312	Best		212	Best			
<i>A. m. var. alba</i>	constrained	3572.4051	96.1739	0.002	237	25	6.38	3.92	< 0.001
<i>A. m. var. formosa</i>	constrained	3656.3632	180.1320	< 0.001	248	36	7.16	5.03	< 0.001
<i>A. m. var. regalis</i>	constrained	3624.9986	148.7674	< 0.001	240	28	6.45	4.34	< 0.001

**Fig. 2** Maximum-parsimony haplotype network constructed based on ITS sequences at 95% connection limit. Gaps were scored as 'new state'. Roman numbers indicate sampled haplotypes, while grey ovals represent unsampled extant or extinct haplotypes. Dotted grey lines indicate connections that were only found at connection limit  $\leq 92\%$ . Haplotypes in bold have been found in Alaska.

rejected ( $P < 0.05$ ) in clade 3-2 and the total cladogram, with significant, large interior clade (I) and interior vs. tip clades (I-T)  $D_n$  values in clade 3-2, and with significant, small tip (T) and I  $D_c$  values and small I-T  $D_n$  value in the total cladogram (Table 3). Based on the most up-to-date (14 July 2004; <http://darwin.uvigo.es/software/geodis.html>) version of the inference key of Templeton (1998), the significant statistical association between haplotype and geography was due to contiguous range expansion (CRE) in the total network of Clade I. There was insufficient information to differentiate between CRE, long-distance colonization (LCD), and past fragmentation (PF) in clade 3-2 (Table 3).

In the network of Clade II, a statistically significant association was found between genotype and geographic origin in clades 2-1 and 2-2. Significant, large I  $D_n$  and I-T  $D_n$ , and significant, small T  $D_c$  and T  $D_n$  values were found in clade 2-1, while significant, small I  $D_c$ , I  $D_n$ , and I-T  $D_n$  values were detected in clade 2-2. Although we were not able to differentiate between allopatric fragmentation (AF) and isolation by distance (IBD) in clade 2-1, CRE was inferred in clade 2-2. Also, we detected significant

genotype–geography association in the total Clade II cladogram with CRE as the underlying mechanism.

The Clade III network contained only a single one-step clade in which significant, large I and I-T  $D_n$  values were detected. However, it was not possible to discriminate between IBD and AF due to the small number of sampled haplotypes.

NCA of the total cladogram containing Clades I, II, and III detected significant, small T  $D_c$  and T  $D_n$ , and significant, large I-T  $D_c$  and I-T  $D_n$  values. The inference that Clade II was the interior clade was justified by the tcs program, which designated haplotype I in Clade II to have the highest outgroup probability that correlates with haplotype age. Allopatric fragmentation was inferred to explain the ancient divergence of *A. muscaria* populations (Table 3). This hypothesis is further supported by the presence of long branches separating the major clades.

#### Coalescent analyses

After removing the indels, seven previously detected haplotypes collapsed, resulting in a total of 18 distinct ITS haplotypes (Table 4). The site compatibility matrix showed



**Table 3** Results of the nested clade analyses. The nested design is given in Fig. 2, as are the haplotype and clade designations. Following the name or number of any given clade are the clade ( $D_c$ ) and nested clade ( $D_n$ ) distances. Also, in those nesting clades containing both tip and interior nested clades, the average difference between interior vs. tip clades for both distance measures is given in the row labelled I-T. Superscripts S and L indicate significantly ( $\alpha = 0.05$ ) small or large values, respectively. At the bottom of the boxes that indicate a nested set of clades in which one or more of the distance measures were significantly large or small, inference key steps and the biological inference are given. The numbers refer to the sequence of questions in the key that the pattern generated, followed by the answer to the final question in the inference key. Abbreviations used are as follows: AF, allopatric fragmentation; CRE, contiguous range expansion; IBD, isolation by distance; LDC, long-distance colonization; PF, past fragmentation. Two or more possible inferences are given when there was insufficient data to infer the single most likely explanation

Haplotype			1-step clade			2-step clade			3-step clade			Species-level clade		
Name	$D_c$	$D_n$	Name	$D_c$	$D_n$	Name	$D_c$	$D_n$	Name	$D_c$	$D_n$	Name	$D_c$	$D_n$
I	0	0	1-1(I)	0	6974 <sup>L</sup>									
II(I)	561	555												
III(T)	0	225												
I-T	561	331	1-3(T)	532 <sup>S</sup>	1397 <sup>S</sup>									
IV	0	0	1-5(T)	0	6974									
V	0	0	1-6(T)	0	6974									
VIII	0	0	1-9(T)	0	2052									
			I-T	-409	4668 <sup>L</sup>									
			1-2-3-4-9-10 No: AF/IBD			2-1(I)	2458 <sup>S</sup>	4724 <sup>S</sup>						
VI(I)	2226	2067												
VII(T)	0	1186												
I-T	2226	880	1-2(I)	1937 <sup>S</sup>	3773 <sup>S</sup>									
XI	0	0	1-4(T)	0	6175									
X	0	0	1-7(T)	0	6175									
			I-T	1937	-2403 <sup>S</sup>									
			1-2-11-12 No: CRE			2-2(T)	4374	7468 <sup>L</sup>						
IX	0	0	1-8	0	0	2-3(T)	0	4310 <sup>S</sup>						
						I-T	-1186	-2218 <sup>S</sup>						
						1-2-11-12 No: CRE						Clade II(I)	5342	5630
XIII	0	0	1-13	0	0	2-6(I)	0	4610						
XIV	0	0												
XV	0	0												
XVI	0	0	1-10(I)	0	123									
XVII(I)	0	49												
XVIII(T)	0	196												
I-T	0	147	1-12(T)	79	123	2-4(T)	123	748						
			I-T	-79	-1	I-T	-123	3861	3-1(T)	1458 <sup>S</sup>	1706			
XII	0	0	1-16	0	0	2-8(I)	0 <sup>S</sup>	2384 <sup>L</sup>						
XIX	0	0	1-17(I)	0	795									
XX	0	0	1-14(T)	0	258									
			I-T	0	537	2-7(T)	392	1119						
XXI	0	0	1-15(I)	0	0									
XXII	0	0	1-11(T)	0	0	2-5(T)	0	1092						
						I-T	-196	1278 <sup>L</sup>						
						1-2-11-12-13-14 Yes: CRE/LDC/PF			3-2(I)	1177 <sup>S</sup>	2735			
									I-T	280	-1028 <sup>S</sup>			
									1-2-11-12 No: CRE			Clade I(T)	2077 <sup>S</sup>	2765 <sup>S</sup>
XXIII(I)	6136	6287 <sup>L</sup>												
XXIV(T)	0	2783												
XXV(T)	0	2783												
I-T	6136	3504 <sup>L</sup>												
1-2-11-17-4-9-10 No: AF/IBD												Clade III(T)	4203	5738
												I-T	2395 <sup>L</sup>	1649 <sup>L</sup>
												1-2-3-4-9 No: AF		

**Table 4** Polymorphic sites in the ITS haplotypes collapsed after removing indels from the original ITS data set for the subsequent coalescent analyses. Position refers to that in the original alignment, site number is the designation of the given mutation as shown on Fig. 3, site type refers to either transition (t) or transversion (v) change with regard to the consensus sequence. Roman numbers refer to haplotype designations on Figs 2 and 3. Haplotypes marked with asterisk include more than one haplotypes from the nested clade analyses, where indels were not excluded

Position	1111122222233444444555666 68995678901247868122367029233 72899049848224345327377164447
Site number	11111111112222222222 12345678901234567890123456789
Site type	ttttvtttvtvtvtttttvvttvtvttt
Character type	-iii-iii-i-i-----iii--i-i---
Consensus	CGCTTGCTGCACAACGTGAAGTGCGCCT
<hr/>	
Haplotype†	
I*	.ATC...C.A.A.....G..T.T...
III	.ATC...CAA.A.....G..T.T...
X	.ATC...C.A.AT.....G..T.T...
VII	.ATC...C.A.A...A...G..T.T...
XI	.ATC...C.A.A...A..G..T.T...
IX	...C...C.A.A.....G..T.T.T.
XXIII	...C.AT...A.....
XXIV	...C.AT...A..T.....
XXV	...C.AT...A.....T.....
XIV	.....C...C.....
XV	...A.....C.....
XX	.....G..G..C.C.....
XVII	T.....CC.....
XVIII	.....CC.....
XXI*	.....C..T.....
XVI	.....C.....T..
XIX	.....C.....
XII*	.....C.....C

†Collapsed haplotypes after removing indels: I\* = I, II, IV, V, VI, VIII; XXI\* = XXI, XXII; XII\* = XII, XIII.

conflict at positions 123–124; therefore these were excluded from subsequent analyses. The coalescent-based ITS genealogy was informative for inferring the mutational history with respect to variation between and within the major clades (Fig. 3). It also confirmed that Clade III likely is the sister clade of Clade I, with a divergence time estimate of 0.939, measured in coalescent units of  $2N$ , where  $N$  is the population size. The mean ages of the first radiation of Clades I, II, and III are 0.128, 0.276, and 0.507, respectively. This suggests that the oldest within-clade radiation may have taken place in Clade III, despite the low number of observed mutations, and that mutation rate in Clade III is much lower than mutation rates observed in the two other clades. Also, Clade I seems the youngest, suggesting that the range expansion in North America likely started more recently than that in Eurasia.

### Molecular clock analyses

ML analyses of the LSU data set conducted with and without the enforcement of a molecular clock resulted in one tree each with likelihood values of  $-\ln L_{\text{clock}} = 2124.1808$  and  $-\ln L_{\text{no clock}} = 2122.2267$ , respectively. Since twice the difference of likelihood scores ( $2 \times 1.9541 = 3.9082$ ) was smaller than the critical  $\chi^2_{\alpha=0.05; d.f.=8} = 15.51$  value, the difference between the trees obtained with and without enforcing the molecular clock is not significant. The age of the first separation within *A. muscaria* (between Clades I and II) was estimated at  $7.48 \pm 4.53$  Ma.

### Discussion

Phylogenies inferred from the individual and combined data sets, and the supertree concordantly suggested three distinct clades in the *Amanita muscaria* species complex. These clades were first detected by Oda *et al.* (2004) and were referred to as geographic groups (i.e. allopatric populations). However, our data suggest that these groups are not entirely allopatric, but have geographic ranges that overlap in Alaska. We found representatives of all three clades in interior Alaska, and specimens from Clades II and III in western arctic Alaska. Because the nonconflicting gene genealogies indicate the lack of gene flow among the clades, we conclude that these groups represent distinct phylogenetic species with sympatric populations in Alaska (Fig. 4A).

Interestingly, all detected phylogenetic species within *A. muscaria* share at least two morphological varieties with other species. Clades I and II both contain at least four (var. *alba*, var. *formosa*, var. *regalis*, var. *muscaria* and/or var. *flavivolvata*), while at least two (var. *regalis*, var. *muscaria* and/or var. *flavivolvata*) have been found to date in Clade III. The most parsimonious explanation for the evolution of these morphological varieties is the presence of ancestral polymorphism in pileus and wart colour that pre-dated the separation of the phylogenetic species. In addition, the pileus colour may be influenced by unknown biotic or abiotic environmental factors. Although different colour varieties generally were found in all sampled climatic zones (temperate, boreal, and arctic-subalpine), eight of the nine *A. muscaria* var. *regalis* specimens were from regions with cold climate (either boreal, arctic or subalpine). The only *A. muscaria* var. *regalis* found in a more temperate climate was the one from the rainforests of southeastern Alaska, only a few miles from the subalpine zone. This finding confirms its rather limited distribution that is restricted to coniferous forests, low arctic and subalpine regions of northern and central Europe, and Alaska (Miller 1982; Jenkins 1986).

It is a widely held assumption that low genetic variation is indicative of recent colonization and that the greatest



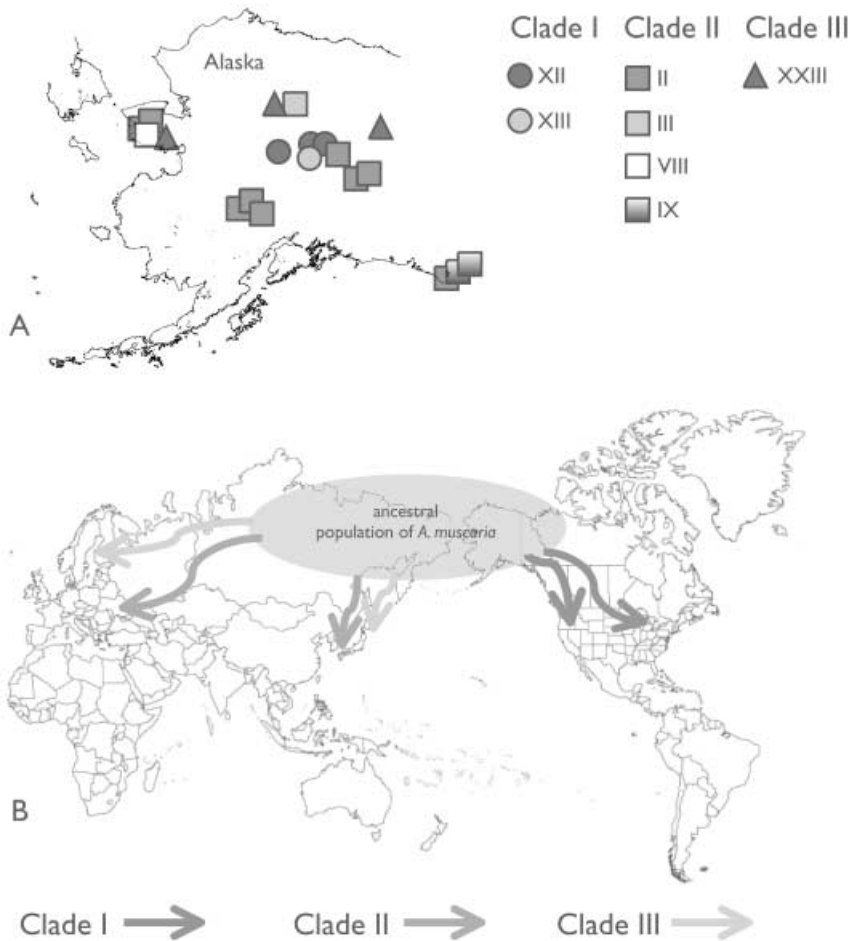


**Fig. 4** (A) Outline map of Alaska showing the geographic distribution of the sampled haplotypes of the three phylogenetic species. (B) Mercator world map showing the putative ancestral population and possible migration routes of the phylogenetic species.

concordantly suggest that the centre of origin of *A. muscaria* likely is in Beringia (Fig. 4B). We hypothesize that the ancestral *A. muscaria* population evolved in the humid, temperate forests that covered much of Beringia in the late Tertiary (Hultén 1968; Graham 1999). Although it is difficult to estimate the divergence times of the major clades due to the wide range of time estimates of our molecular clock analyses ( $7.48 \pm 4.53$  Ma), the fragmentation of the ancestral population into at least two major clades might have taken place as a consequence of the opening of the Bering Strait about 12 Ma. Clade III likely is a sister group of Clade I, as inferred from the phylogenetic and coalescent analyses, and it is safe to conclude that the ancestral population was divided into Eurasian and Alaskan populations. With the cooling climate, some populations of Clades I and II likely migrated southward in North America and Eurasia (Fig. 3B), respectively, as is supported by the contiguous range expansion inferred in both clades by NCA. However, coalescent mutation age estimates suggest that the radiation and southward expansion may have happened more recently in North America (Clade I) than in Eurasia (Clades II and III).

In North America, the expansion of Clade I took two main directions: (i) southward along the western side the Rocky Mountains which resulted in the extant populations in the western United States, represented by samples from California and Idaho; and (ii) southeastward along the eastern slopes of the Rocky Mountains which allowed the establishment of populations in the eastern United States, represented by samples from Massachusetts and New York. This latter route was shared by numerous plant taxa that originated in Alaska and replaced many species along their migration to the southeast (Budantsev 1992). Interestingly, we did not find any haplotype in Alaska that descended from other North American haplotypes. This suggests that populations of *A. muscaria* survived the glacial maxima in Alaskan refugia and there was no significant postglacial migration from southern populations back to Alaska. On the contrary, Alaskan populations likely gave rise to both eastern and western North American lineages before the Quaternary period.

Range expansion patterns in Clades II and III are more difficult to interpret, partly because of large unsampled areas in Asia. The NCA results in clade 2-1, which is the



interior clade and the only one containing both Alaskan and Eurasian samples, indicate allopatric fragmentation or isolation by distance. Isolates from unsampled areas in Asia are needed to clarify this question. However, a more basal bifurcation, separating the southeast Alaskan group (II/A, ITS haplotype IX) from the rest of Clade II, can be observed in the combined phylogeny and the coalescent-based genealogy. It is somewhat surprising that no evidence was found for migrations of *A. muscaria* from Eurasia to North America/Alaska, despite what had been suggested by Oda *et al.* (2004). This question should be addressed by further phylogeographic studies with increased sample size.

Beside the southward range expansions detailed above, populations of all three species clades have continuously inhabited Beringia. In the Quaternary, the Illinoian and Wisconsinian glaciations likely restricted *A. muscaria* to isolated refugia of boreal forest and shrub tundra along the Yukon and Tanana rivers in interior Alaska that remained unglaciated (Hultén 1968; Graham 1999). While it is unclear whether conifers were present in the region at glacial maxima, it is very likely that *Betula*, *Dryas*, *Populus* and *Salix* inhabited at least some parts of the region (Edwards *et al.* 2000; Swanson 2003) and likely were able to maintain refugia of *A. muscaria*. The ecological plasticity of *A. muscaria*, i.e. the broad range of potential mycorrhizal hosts, including *Betula*, *Dryas* and *Salix* spp. in subalpine tundra (Miller 1982), supports the hypothesis of glacial refugia in Alaska. In addition, although earlier pollen data did not indicate the presence of *Picea* in Beringia at the last glacial maximum (Edwards *et al.* 2000; Swanson 2003), recent pollen data (Brubaker *et al.* 2005) and phylogeographic analyses based on DNA sequences (F.S. Hu, personal communication) suggest the existence of glacial refugia of *P. glauca* and *P. mariana* in eastern Beringia.

In this study, we documented the existence of three distinct phylogenetic species in the *A. muscaria* species complex. Furthermore, we hypothesized evolutionary and phylogeographic processes leading to speciation and intraspecific population structures. Future studies should include specimens from unsampled regions to further elucidate the phylogeography of the species complex. Among these, Siberia is of particular interest, because it might possess genetically diverse populations, including putatively ancestral Beringian elements.

The implications of our results are not restricted to *A. muscaria*. The phylogeographic patterns seen here might be shared, at least in part, by many boreal ECM fungi in the Northern Hemisphere, particularly in North America. It is certain that many plant lineages contributing to the recent boreal and temperate flora evolved within high-latitude forests of Beringia during the Tertiary and migrated southward as the climate cooled (Graham 1999). Furthermore, because there is increasing evidence for boreal forest glacial refugia in Alaska, Holocene migrations of boreal plants

and ECM fungi likely occurred not only northward from southern refugia, but southeastward from Alaskan refugia. This is supported by the rapid postglacial colonization of the present boreal regions by *Picea*, and the fact that no recent migration of *A. muscaria* from more southern regions of North America to Alaska was detected in our analyses. As a consequence, we propose that Beringia is not only the original and longest inhabited region for many plant and animal taxa, but may represent a biodiversity 'hotspot' for high-latitude ECM fungi as well.

## Acknowledgements

This research is part of the Metagenomics of Boreal Forest Fungi project (NSF grant no. 0333308) to D.L. Taylor, G.A. Laursen and others. J. Geml is grateful to Deep Hypha (NSF 0090301) for continued research coordination support. Research support was also provided in part by National Park Service grants (nos PX9830-93-062, PX9830-92-385, PX9830-0-0451, PX9830-0-0472, and PX9830-0-0512) and the UAF Cooperative Extension Service under UAA Sustainable Development grant no. G000000268 as sub-grant no. 65089-360163 made to the secondary author. The authors also thank Thomas Marr, James Long, and Shawn Houston at the Bioinformatics Core at UAF, Institute of Arctic Biology, for the technical support in phylogenetic analyses. Special thanks go to Thomas Marr for his suggestions on the initial manuscript, and to Ignazio Carbone for his help with the coalescent analyses. This work was also supported by the Alaska EPSCoR (NSF grant no. EPS-0346770) and the Alaska INBRE (NIH NCCR grant no. 2P20RR16466).

## Supplementary material

The supplementary material is available from <http://www.blackwellpublishing.com/products/journals/suppmat/MEC/MEC2799/MEC2799sm.htm>

**Fig. S1** Supertree constructed by the matrix representation with parsimony method.

## References

- Adams JM, Faure H (1997) Preliminary vegetation maps of the world since the last glacial maximum: an aid to archaeological understanding. *Journal of Archaeological Science*, **24**, 623–647.
- Archie JW (1989) A randomization test for phylogenetic information in systematic data. *Systematic Zoology*, **38**, 239–252.
- Aylor D, Carbone I (2003) *SNAP Combine and MAP*. Department of Plant Pathology, North Carolina State University, Raleigh, North Carolina. ([www.cals.ncsu.edu/plantpath/faculty/carbone/home.html](http://www.cals.ncsu.edu/plantpath/faculty/carbone/home.html)).
- Bagley SJ, Orlovich DA (2004) Genet size and distribution of *Amanita muscaria* in a suburban park, Dunedin, New Zealand. *New Zealand Journal of Botany*, **42**, 939–947.
- Baum BR (1992) Combining trees as a way of combining data sets for phylogenetic inference, and the desirability of combining gene trees. *Taxon*, **41**, 3–10.
- Beerli P, Felsenstein J (1999) Maximum-likelihood estimation of migration rates and effective population numbers in two populations using a coalescent approach. *Genetics*, **152**, 763–773.

- Benedict RG (1966) Chemotaxonomic significance of isoxazole derivatives in *Amanita* species. *Lloydia*, **29**, 333–342.
- Benjamin DR (1995) *Mushrooms: Poisons and Panaceas*. W.H. Freeman, San Francisco, California.
- Berbee ML, Taylor JW (2001) Fungal molecular evolution: gene trees and geologic time. In: *The Mycota VII, Part B, Systematics and Evolution* (eds McLaughlin DJ, McLaughlin EG, Lemke PA), pp. 229–245. Springer-Verlag, Berlin, Germany.
- Bhatt RP, Tulloss RE, Semwal KC *et al.* (2003) *Amanitaceae* reported from India. A critically annotated checklist. *Mycotaxon*, **88**, 249–270.
- Bininda-Emonds ORP, Sanderson MJ (2001) Assessment of the accuracy of matrix representation with parsimony analysis supertree construction. *Systematic Biology*, **50**, 565–579.
- Brubaker LB, Anderson PM, Edwards ME, Lozhkin AV (2005) Beringia as a glacial refugium for boreal trees and shrubs: new perspectives from mapped pollen data. *Journal of Biogeography*, **32**, 833–848.
- Budantsev LY (1992) Early stages of formation and dispersal of the temperate flora in the boreal region. *Botanical Review*, **58**, 1–48.
- Carbone I, Liu YC, Bradley IH, Milgroom MG (2004) Recombination and migration of *Cryphonectria hypovirus 1* as inferred from gene genealogies and the coalescent. *Genetics*, **166**, 1611–1629.
- Clement M, Posada D, Crandall KA (2000) tcs: a computer program to estimate gene genealogies. *Molecular Ecology*, **9**, 1657–1659.
- Crandall KA (1996) Multiple interspecies transmissions of human and simian T-cell leukemia/lymphoma virus type I sequences. *Molecular Biology and Evolution*, **13**, 115–131.
- Creevey CJ, McInerney JO (2004) CLANN: investigating phylogenetic information through supertree analyses. *Bioinformatics*, **21**, 390–392.
- Edwards ME, Anderson PM, Brubaker LB *et al.* (2000) Pollen-based biomes for Beringia 18 000, 6000 and 0 <sup>14</sup>C yr BP. *Journal of Biogeography*, **27**, 521–554.
- Elias SA (2000) Late Pleistocene beetle faunas of Beringia: where east met west. *Journal of Biogeography*, **27**, 1349–1363.
- Faith DP, Cranston PS (1991) Could a cladogram this short have arisen by chance alone? On permutation tests for cladistic structure. *Cladistics*, **7**, 1–28.
- Felsenstein J (1985) Confidence limits on phylogenies: an approach using the bootstrap. *Evolution*, **39**, 783–791.
- Fu YX, Li WH (1993) Maximum likelihood estimation of population parameters. *Genetics*, **134**, 1261–1270.
- Gardes M, Bruns TD (1993) ITS primers with enhanced specificity of basidiomycetes: application to the identification of mycorrhizae and rusts. *Molecular Ecology*, **2**, 113–118.
- Graham A (1999) *Late Cretaceous and Cenozoic History of North American Vegetation*. Oxford University Press, Oxford and New York.
- Griffiths RC, Tavaré S (1994) Ancestral inference in population genetics. *Statistical Sciences*, **9**, 307–319.
- Hey J, Wakeley J (1997) A coalescent estimator of the population recombination rate. *Genetics*, **145**, 833–846.
- Hudler GW (1998) *Magical Mushrooms, Mischievous Molds*. Princeton University Press, Princeton, New Jersey, and Oxford, UK.
- Huelsenbeck JP, Ronquist F (2001) MRBAYES: Bayesian inference of phylogenetic trees. *Bioinformatics*, **17**, 754–755.
- Hultén E (1968) *Flora of Alaska and Neighboring Territories*. Stanford University Press, Stanford, California.
- Jenkins DT (1986) *Amanita of North America*. Mad River Press, Eureka, California.
- Jenkins DT, Petersen RH (1976) A neotype specimen for *Amanita muscaria*. *Mycologia*, **68**, 463–469.
- Jones KE, Purvis A, MacLarnon A, Bininda-Emonds ORP, Simmons NB (2002) A phylogenetic supertree of the bats (Mammalia: Chiroptera). *Biological Reviews*, **77**, 223–259.
- Kaufman DS, Ager TA, Anderson NJ *et al.* (2004) Holocene thermal maximum in the western Arctic (0–180°W). *Quaternary Science Reviews*, **23**, 529–560.
- Kishino H, Hasegawa M (1989) Evaluation of the maximum likelihood estimate of the evolutionary tree topologies from DNA sequence data, and the branching order of the Hominoidea. *Journal of Molecular Evolution*, **29**, 170–179.
- Lutzoni F, Wagner W, Reeb V, Zoller S (2000) Integrating ambiguously aligned regions of DNA sequences in phylogenetic analyses without violating positional homology. *Systematic Biology*, **49**, 628–651.
- MacNeil D, Strobeck C (1987) Evolutionary relationships among colonies of Columbian ground squirrels as shown by mitochondrial DNA. *Evolution*, **41**, 873–881.
- Markwordt J, Doshi R, Carbone I (2003) *SNAP Clade and Matrix*. Department of Plant Pathology, North Carolina State University, Raleigh, North Carolina. ([www.cals.ncsu.edu/plantpath/faculty/carbone/home.html](http://www.cals.ncsu.edu/plantpath/faculty/carbone/home.html)).
- Michelot D, Melendez-Howell LM (2003) *Amanita muscaria*: chemistry, biology, toxicology, and ethnomycology. *Mycological Research*, **107**, 131–146.
- Miller OK (1982) Higher fungi in Alaskan subarctic tundra and taiga plant communities. In: *Arctic and Alpine Mycology: the First International Symposium on Arcto-Alpine Mycology* (eds Laursen GA, Ammirati JF), pp. 123–149. University of Washington Press, Seattle and London.
- Nielsen R, Wakeley J (2001) Distinguishing migration from isolation: a Markov chain Monte Carlo approach. *Genetics*, **158**, 885–896.
- Oda T, Tanaka C, Tsuda M (2004) Molecular phylogeny and biogeography of the widely distributed *Amanita* species, *A. muscaria* and *A. pantherina*. *Mycological Research*, **108**, 885–896.
- Page RDM, Holmes EC (1998) *Molecular Evolution – A Phylogenetic Approach*. Blackwell Science, Oxford, UK.
- Pérez-Silva E, Herrera T (1991) *Iconografía de Macromicetos de México. Publicaciones Especiales 6*. Universidad Nacional Autónoma de México, Instituto de Biología.
- Posada D, Crandall KA (1998) MODELTEST: testing the model of DNA substitution. *Bioinformatics*, **14**, 817–818.
- Posada D, Crandall KA, Templeton AR (2000) GEODIS: a program for the cladistic nested analysis of the geographical distribution of genetic haplotypes. *Molecular Ecology*, **9**, 487–488.
- Qian H (1999) Floristic analysis of vascular plant genera of North America north of Mexico: characteristics of phytogeography. *Journal of Biogeography*, **26**, 1307–1321.
- Ragan MA (1992) Phylogenetic inference based on matrix representation of trees. *Molecular Phylogenetics and Evolution*, **1**, 53–58.
- Reid DA (1980) A monograph of the Australian species of *Amanita* Persoon ex Hooker (Fungi). *Australian Journal of Botany*, **8**, 1–96.
- Reid DA, Eicker A (1991) South African fungi: the genus *Amanita*. *Mycological Research*, **95**, 80–95.
- Reiss AR, Ashworth AC, Schwert DP (1999) Molecular genetic evidence for the post-Pleistocene divergence of populations of the arctic-alpine ground beetle *Amara alpina* (Paykull) (Coleoptera: Carabidae). *Journal of Biogeography*, **26**, 785–794.
- Ridley GS (1991) The New Zealand species of *Amanita* (Fungi: Agaricales). *Australian Systematic Botany*, **4**, 325–354.

- Rimóczi I (1994) Nagygyombáink cönológiai és ökológiai jellemzése. *Mikológiai Közlemények*, **33**, 4–150.
- Rozas J, Rozas R (1999) DNASP version 3: an integrated program for molecular population genetics and molecular evolution analysis. *Bioinformatics*, **15**, 174–175.
- Sanderson MJ, Purvis A, Henze C (1998) Phylogenetic supertrees: assembling the trees of life. *Trends in Ecology & Evolution*, **13**, 105–109.
- Santiago C, Cifuentes J, Villegas M (1984) Contribution to the knowledge of *Amanita* subgenus *Amanita* in Mexico. *Boletín de la Sociedad Mexicana de Micología*, **19**, 93–105.
- Schneider S, Roessli D, Excoffier L (2000) *ARLEQUIN (Version 2.000): A software for population genetics data analysis*. Genetics and Biometry Laboratory, Department of Anthropology, University of Geneva, Switzerland.
- Sperling FH, Harrison RG (1994) Mitochondrial DNA variation within and between species of the *Papilio machaon* group of swallowtail butterflies. *Evolution*, **48**, 408–422.
- Swanson DK (2003) A comparison of taiga flora in north-eastern Russia and Alaska/Yukon. *Journal of Biogeography*, **30**, 1109–1121.
- Swofford DL (2002) *PAUP\*. Phylogenetic Analysis Using Parsimony (\*and Other Methods)*, 4.0b4a. Sinauer Associates, Sunderland, Massachusetts.
- Tajima F (1989) Statistical method for testing the neutral mutation hypothesis by DNA polymorphism. *Genetics*, **123**, 585–595.
- Tamura K, Nei M (1993) Estimation of the number of nucleotide substitutions in the control region of mitochondrial DNA in humans and chimpanzees. *Molecular Biology and Evolution*, **10**, 512–526.
- Tan HC, Wu RJ (1986) The ecological and geographical distribution of 108 species of macromycetes from the subtropical, evergreen, broad-leaved forests in China. *Mycotaxon*, **25**, 183–194.
- Taylor JW, Jacobson DJ, Kroken S *et al.* (2000) Phylogenetic species recognition and species concepts in fungi. *Fungal Genetics and Biology*, **31**, 21–32.
- Templeton AR (1998) Nested clade analyses of phylogeographic data: testing hypotheses about gene flow and population history. *Molecular Ecology*, **7**, 381–397.
- Thiers HD (1982) *The Agaricales of California: 1. Amanitaceae*. Mad River Press, Eureka, California.
- Thompson JD, Gibson TJ, Plewniak F, Jeanmougin F, Higgins DG (1997) The CLUSTAL\_X Windows interface: flexible strategies for multiple sequence alignment aided by quality analysis tools. *Nucleic Acids Research*, **25**, 4876–4882.
- Trappe JM (1962) Fungus associates of ectotrophic mycorrhiza. *Botanical Review*, **28**, 538–606.
- Tulloss RE, Stephenson SL, Bhatt RP, Kumar A (1995) Studies of *Amanita* (Amanitaceae) in West Virginia and adjacent areas of the mid-Appalachians. Preliminary results. *Mycotaxon*, **56**, 243–293.
- White TJ, Bruns T, Lee S, Taylor JW (1990) Amplification and direct sequencing of fungal ribosomal RNA genes for phylogenetics. In: *PCR Protocols: A Guide to Methods and Applications* (eds Innis MA, Gelfand DH, Sninsky JJ, White TJ), pp. 315–322. Academic Press, New York.
- Yang Z (1997) PAML: a program package for phylogenetic analysis by maximum likelihood. *CABIOS*, **13**, 555–556.

---

Dr. Geml is interested in the systematics, evolution and biogeography of ectomycorrhizal Basidiomycota, particularly in Beringia. Dr. Laursen has carried out a 37-year study of high latitude fungal taxonomy, morphology and ecological relationships of the higher fungi within extreme environments. He has developed an herbarium of approximately 18,900 fungal, lichen and moss collections, creating a valuable genomic resource for further studies. The Taylor lab seeks to understand the ecological and evolutionary dynamics of plant-fungal interactions, with emphases on ectomycorrhizae and orchid mycorrhizae, and also uses metagenomics approaches to better understand the diversity and function of boreal forest fungi.

---